SUPPLEMENTARY DISCUSSION

It is possible that melts from (Fe,Ni) metal–saturated sources can be recognized by their olivine compositions. Out of all transition metal oxides in olivine, NiO is most easily reduced to metal when fO_2 falls, followed by CoO and FeO. The sequence of reduction follows broadly the electromotive series. Therefore, a melt that is generated in equilibrium with an (Fe,Ni) metal phase may contain olivines that have unusually low NiO concentrations at slightly lower CoO and FeO. Examples are olivines from lunar basalts[33,34] and olivines from melts that experienced reduction because they became contaminated with organic carbon[35]. Suppl. Fig. S1 summarizes compositions of olivine phenocrysts from two samples of Karoo picrites from southern Malawi[36]. The majority of grains have normal to high NiO concentrations around 3500 ppm, and Ni/Co ratios of 18 to 20. Both NiO and Ni/Co show the usual decline in concentration with increasing fayalite (Fe_2SiO_4) component, consistent with a magmatic differentiation trend. The cores of some primitive olivines, however, have NiO concentrations as low as 300 ppm and Ni/Co atomic ratios of ~ 5, defining what is termed in Suppl. Fig. S1a an oxidation trend. Usually, low–NiO compositions are only preserved in cores of phenocrysts, and they are overgrown by rims rich in NiO and slightly enriched in CoO and FeO. Obviously, if metal–saturated conditions were responsible they could have prevailed only in the very early stages of melt generation. No metal inclusions have yet been identified in these olivines, so the ultimate test for our proposal of metal saturation still is missing. None the less, low NiO and Ni/Co at slightly lowered fayalite are signatures expected with metal saturation. It might be worthwhile in future to analyze more systematically olivine populations in primitive melts generated at great depths, to test how widespread these signatures are and whether they correlate with the depth of melting.

33. Karner, J., Papike, J. J. & Shearer, C. K. Olivine from planetary basalts; chemical signatures that indicate planetary parentage and those that record igneous setting and process. *Am. Mineral.* **88**, 806–816 (2003).
34. Papike, J. J., Fowler, G. W., Adcock, C. T, & Shearer, C. K. Systematics of Ni and Co in olivine from planetary melt systems: Lunar mare basalts. *Am. Mineral.* **84**, 392–399 (1999).
35. Pedersen A. K. Basaltic glass with hightemperature equilibrated immiscible sulphide bodies with native iron from Disko, central west Greenland. *Contrib. Mineral. Petrol.* **69**, 397–407 (1979).
36. Woolley, A. R., Bevan, J. C., Elliott, C. J. The Karroo dolerites of southern Malawi and their regional geochemical implications. *Mineral. Mag.* **43**, 487–495 (1979).
37. Sobolev A. V., et al. Estimating the amount of recycled crust in sources of mantle-derived melts. *Science* **316**, 412–417 (2007).

Figure S1

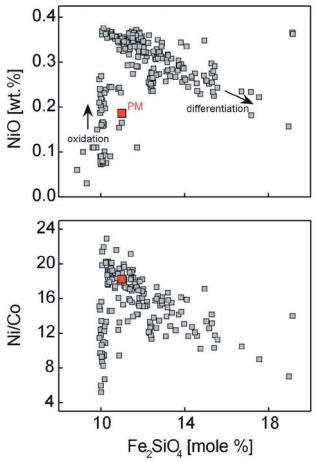

Figure S1: NiO contents and Ni/Co atomic ratios of olivines in the Karoo picrite sample P23-9 (ref. 35). Superimposed a putative metal oxidation trend (i.e., increasing NiO and Ni/Co at constant FeO) followed by a magmatic differentiation trend. Primitive mantle (PM) values are taken from Palme & O'Neill[15]. Analyses with the JEOL JXA– 8200 Superprobe at Max Planck Institute for Chemistry in Mainz, with some additional Ni analyses performed at the University of Cologne. Analytical conditions were 20 kV/300 nA with 120 sec on peak and background[37].

Table S1: Starting composition and representative electron microprobe analyses of run products.

		exp-10	exp-15	exp-15	zuII-4	zuII-4	zuIII-1	zuIII-1	zu-8	zu-8	zuII-3	zuII-3	zuIV-1	zuIV-1	zuIII-4
pressure (GPa)		1	3	3	6	6	7	7	8	8	10	10	12	12	14
temperature (°C)		1220	1400	1400	1400	1400	1450	1450	1650	1650	1500	1500	1500	1500	1500
run time (h)		48	24	24	4.5	4.5	6	6	1.5	1.5	3.5	3.5	10	10	4.5
ΔfO_2 (IW)		- 0.6(3)	- 0.5(3)	- 0.5(3)	- 0.5(3)	- 0.5(3)	- 0.6(3)	- 0.6(3)	- 1.1(3)	- 1.1(3)	- 0.7(1)	- 0.7(1)	-0.7(2)	-0.7(2)	- 1.3(3)
phase	start. comp.	cpx	grt	cpx	grt	cpx	grt	cpx	grt	cpx	grt	cpx	grt	cpx	grt
SiO_2	47.5	48.8	39.4	50.6	40.4	52.3	40.6	51.8	43.9	54.8	43.5	52.3	43.8	52.7	50.5
TiO_2	0.29	0.18	0.56	0.28	0.81	0.20	0.70	0.23	0.40	0.11	0.68	0.16	0.46	0.16	0.36
Al_2O_3	6.45	4.76	21.2	4.38	20.7	2.45	18.3	2.78	18.1	2.12	15.2	1.50	14.0	1.63	8.40
Cr_2O_3	0.56	0.74	1.30	0.50	1.26	0.36	1.02	0.34	0.96	0.27	0.87	0.29	1.10	0.33	0.69
FeO[a]	26.2	26.4	23.6	24.0	25.0	26.5	23.4	22.7	13.7	13.1	22.1	23.5	20.3	19.7	9.77
Fe_2O_3[a]	–	0.3	1.38	0.82	1.16	0.09	2.26	1.05	2.68	1.10	3.67	3.23	4.61	3.26	5.59
MgO	14.7	13.5	9.21	14.2	9.93	14.9	11.4	15.3	18.4	21.5	12.9	15.6	12.4	15.3	19.4
CaO	3.80	6.01	4.01	4.10	3.82	4.34	3.10	4.43	3.41	6.44	2.91	4.46	2.72	5.11	5.25
Na_2O	0.50	0.16	0.03	0.85	0.04	0.67	0.16	1.18	0.19	1.01	0.14	0.74	0.32	1.15	1.56
Total	100.0	100.9	100.7	99.7	102.0	101.8	100.9	99.8	101.7	100.5	102.0	101.8	99.7	99.3	101.5
Mg/(Mg+Fe)[a]	0.5	0.48(1)	0.41(1)	0.51(1)	0.41(1)	0.50(1)	0.47(1)	0.55(1)	0.71(3)	0.75(2)	0.51(3)	0.54(2)	0.52(1)	0.58(1)	0.78(2)
$Fe^{3+}/\Sigma Fe$ (EELS)		0.01(3)	0.05(3)	0.03(3)	0.04(2)	0.00(3)	0.08(3)	0.04(3)	0.15(4)	0.07(3)	0.13(2)	0.11(3)	0.17(5)	0.13(4)	0.34(6)
Si (per formula unit)		1.88(1)	3.01(1)	1.93(2)	3.06(2)	1.98(1)	3.11(2)	1.97(1)	3.18(2)	2.00(1)	3.28(2)	1.99(1)	3.36(2)	2.02(1)	3.67(1)
Al (per formula unit)		0.22(2)	1.91(2)	0.20(2)	1.76(2)	0.11(1)	1.65(4)	0.13(1)	1.55(2)	0.09(1)	1.35(3)	0.07(1)	1.27(1)	0.07(1)	0.72(3)

Uncertainties in parenthesis are standard errors of the mean (95% confidence). (a) Recalculated based on $Fe^{3+}/\Sigma Fe$ ratio (EELS). Electron microprobe analyses at 15 kV and 15 nA using natural silicates as standards. Run products were thinned to electron transparency with a Gatan Duo-Mill ion milling system. Pyroxene, garnet, and majorite$_{ss}$ were analyzed for $Fe^{3+}/\Sigma Fe$ ratios with a Zeiss Libra 200 FE transmission electron microscope equipped with an in-column Omega energy filter and operated at 200 kV. The energy resolution was about 1 eV, measured as full width at half maximum of the zero loss peak. Molar $Fe^{3+}/\Sigma Fe$ was calculated from the iron $L_{2/3}$ spectra using the calibration of van Aken & Liebscher[16]. Background subtraction followed the procedure described by van Aken et al.[17]. fO_2 values calculated from ferrosilite (in cpx) and almandine (in grt) activities using ideal ionic solution models. Note that the 8 GPa and 14 GPa runs may have suffered some melt loss at run conditions, causing silicates to be more magnesian and Mg/(Mg+Fe) atomic ratios more variable. In the high pressure runs > 8 GPa some chemical variation may also be owed to the small amount of starting material (~ 5 mg) that can be equilibrated (c.f. elevated sodium content in grt at 14 GPa).